

2MASS J22521073–1730134: A RESOLVED L/T BINARY AT 14 PARSECS¹

I. NEILL REID AND E. LEWITUS

Space Telescope Science Institute, 3700 San Marin Drive, Baltimore, MD 21218; inr@stsci.edu

AND

ADAM J. BURGASSER^{2,3,4} AND K. L. CRUZ^{4,5}

Department of Astrophysics, American Museum of Natural History, Central Park West at 79th Street, New York, NY 10024;
ajb@mit.edu, kelle@amnh.edu

Received 2005 August 1; accepted 2005 November 7

ABSTRACT

NICMOS images of the nearby late-type L dwarf 2MASS J22521073–1730134 (DENIS-P J225210.73–173013.4) show that it is a close double, separation $0''.13$. The companion is 1.0 mag fainter than the primary in the F110W passband and 1.55 mag fainter in the F170M images. The latter passband is centered on the $1.6\ \mu\text{m}$ methane band. The small separation and the absence of an optical counterpart suggest that the two sources are associated; the relatively blue infrared color suggests that 2MASS J22521073–1730134B is a T-type binary companion of the late-L primary. This hypothesis is supported by infrared spectroscopy, which shows weak methane absorption in both the H and K passbands. We estimate a distance of $13.6^{+3.8}_{-2.6}$ pc to the system and a projected linear separation of 1.75 AU. We consider the potential for measuring dynamical masses of the two components.

Subject headings: binaries: visual — stars: individual (2MASSW J22521073–1730134) — stars: low-mass, brown dwarfs

1. INTRODUCTION

Binary systems play a vital role in astrophysics, notably by providing the main means of measuring masses for individual stars and brown dwarfs. This role is particularly crucial below the hydrogen-burning limit, where rapid evolution and the near coincidence of tracks on the H-R diagram rules out the possibility of estimating masses from statistical calibrations. Recent surveys show that $\sim 15\%$ of ultracool dwarfs (spectral types later than M7) are binaries, with most systems having separations less than ~ 15 AU (Reid et al. 2001b; Bouy et al. 2003; Burgasser et al. 2003b; Gizis et al. 2003). Several systems have periods less than 20 yr and are being monitored astrometrically. To date, dynamical mass estimates have been derived for the M8.5/M9 close binary Gl 569B (Zapatero Osorio et al. 2004), and for the L0.5 binary 2MASSW J0746425+200321 (Bouy et al. 2004; but see Gizis & Reid 2006).

We are currently using high-resolution imaging to search for binary systems among the L dwarfs identified in our census of ultracool dwarfs within 20 pc of the Sun (Cruz et al. 2003; Cruz et al. 2006, in preparation). As part of this project, we recently obtained near-infrared observations of 2MASSW J22521073–1730134 (hereafter simply 2M2252) with the Near-Infrared Camera and Multi-Object Spectrometer (NICMOS) on the *Hubble Space Telescope* (*HST*). This object was identified independently as a nearby ultracool dwarf by Kendall et al. (2004),

based on follow-up observations of candidates from the DENIS survey. Designating it DENIS-P J225210.73–173013.4, Kendall et al. (2004) estimate a spectral type of L7.5 from near-infrared spectroscopy and a distance of 8.3 ± 0.6 pc. Our NICMOS observations resolve 2M2252 into two components with a significantly larger magnitude difference at $1.7\ \mu\text{m}$ than at $1.1\ \mu\text{m}$. Moreover, ground-based near-infrared spectroscopy shows mild methane absorption in both the H and K passbands. This suggests that the companion is a T dwarf. The following section describes the NICMOS imaging and the Infrared Telescope Facility (IRTF) near-infrared spectroscopy, § 3 summarizes the likely properties of the 2M2252 system, and § 4 discusses the implications.

2. OBSERVATIONS

2.1. NICMOS Images

Images of 2M2252 were obtained at 20:20 UT on 2005 June 21 with the NIC1 camera of the *HST* NICMOS instrument as part of our Cycle 13 SNAPSHOT program. The source was observed in the F110W and F170M filters. In both cases, the observations consist of a pair MULTIACCUM exposures, nodding $2''$ between the two exposures. The total exposure times are 284 s at F110W and 896 s in the F170M filter. The data were processed through the standard *HST* pipeline, and Figure 1 shows the F110W and F170M images. 2M2252 is clearly resolved into two components. We used iterative point-spread function (PSF) fitting routines, as described by Burgasser et al. (2003b), to derive a separation of $0''.130 \pm 0''.002$ at position angle $-9^\circ 6' \pm 1''.2$ (measured north through east).

Both sources have image profiles consistent with a point source; the measured full-width half-maxima are 2.6 pixels ($0''.11$) in F110W and 3.4 pixels ($0''.145$) in F170M. 2M2252 lies at moderately high Galactic latitude, $b = -60^\circ 9'$, and there are no other sources within the $11'' \times 11''$ field of view. Thus, if the fainter object is a background source, the a priori probability of it lying within $0''.13$ of the ultracool dwarf is 4×10^{-4} . As

¹ Based on observations made with the NASA/ESA *Hubble Space Telescope*, obtained from the Space Telescope Science Institute, which is operated by the Association of Universities for Research in Astronomy, Inc., under NASA contract NAS 5-26555.

² Current address: Department of Physics, Massachusetts Institute of Technology, 77 Massachusetts Avenue, Cambridge, MA 02139.

³ Spitzer Fellow.

⁴ Visiting astronomer at the Infrared Telescope Facility, which is operated by the University of Hawaii under Cooperative Agreement NCC 5-538 with the National Aeronautics and Space Administration, Office of Space Science, Planetary Astronomy Program.

⁵ NSF Astronomy and Astrophysics Postdoctoral Fellow.

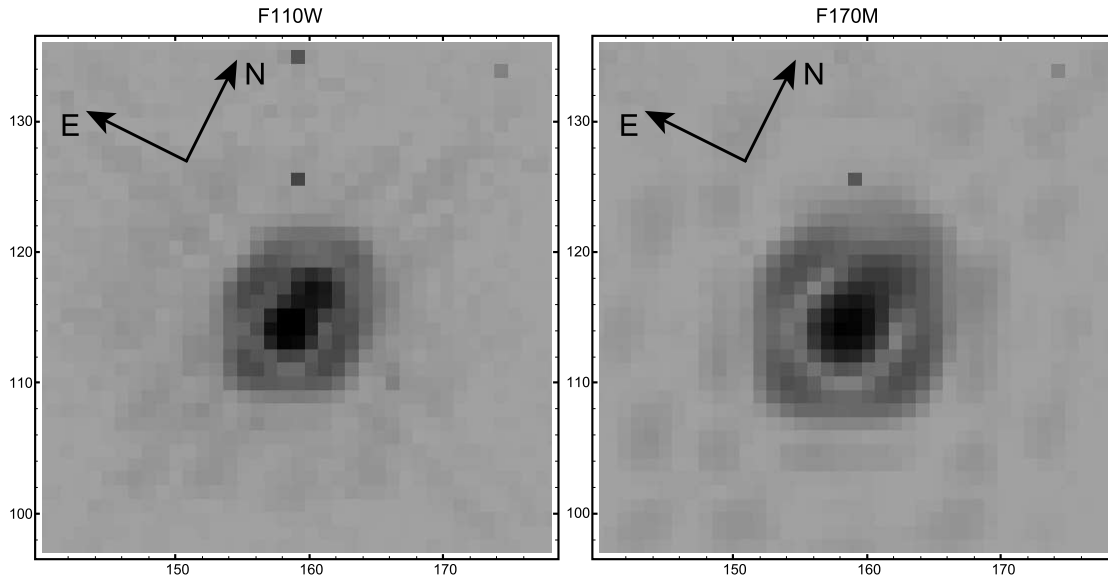


FIG. 1.—NIC1 images of 2M2252; the binary nature of the source is clear. The left panel shows the F110W image with the superimposed axes north and east; the right panel shows the F170M image. The magnitude difference between the two components is larger at the longer wavelength.

discussed further below, our photometric and spectroscopic results favor association, and we therefore refer to the two sources as 2M2252A and 2M2252B.

2.2. Photometry

Figure 1 suggests that the magnitude difference between 2M2252A and 2M2252B is greater in F170M than in the F110W passband. We have quantified this through photometry of the two sources. This requires some care, since the separation of the components is such that 2M2252B overlies the first Airy ring of 2M2252A in both filters. We have dealt with this by using NIC1 observations of 2MASS J004521.4+163445 (2M0045), obtained on 2005 June 23, as a template for both PSFs. 2M0045, an L0 dwarf, is unresolved by NICMOS. We have used the IMSHIFT IRAF routine to align the appropriate 2M0045 image with each 2M2252 component, scaled the 2M0045 data to match the peak flux, and subtracted the images, leaving a “cleaned” image of either 2M2252A or 2M2252B. Although the 2M0045 and 2M2252 observations were separated by only a few days, the PSF profiles are not exactly identical; as a result, the cleaned images of 2M2252B (i.e., the images in which 2M2252A has been removed using the scaled 2M0045 data) exhibit low-level residuals from the subtraction, particularly in F110W.

We have used two techniques to determine relative magnitudes of 2M2252A and 2M2252B from the cleaned images. First, we have measured the peak flux of each component using the IRAF IMEXAM profile-fitting routine; we find a ratio A/B of 2.5 ± 0.2 (1.0 ± 0.08 mag) in the F110W filter and 4.1 ± 0.25 (1.53 ± 0.07 mag) in F170M, where we give the formal uncertainties. We have derived aperture photometry for the 2M2252 system using the IRAF DAOPHOT package, setting an aperture size of radius 15 pixel ($0''.645$). Scaling to Vega magnitudes using the standard *HST* flux calibration and flux zero points of 1786 and 946 Jy at F110W and F170M, respectively, gives apparent magnitudes of $m_{110} = 15.08 \pm 0.03$ and $m_{170} = 13.46 \pm 0.03$. The corresponding magnitudes for the two components are $m_{110} = 15.4 \pm 0.1$ and $m_{170} = 13.7 \pm 0.1$ for 2M2252A and $m_{110} = 16.4 \pm 0.15$ and $m_{170} = 15.1 \pm 0.1$ for 2M2252B.

We have also used DAOPHOT to determine aperture photometry of each source from the PSF-subtracted images. Given the presence of residuals from the subtraction process, the measurements are made with an aperture of radius 3 pixels ($0''.13$). Based on those data, we derive a magnitude difference of 1.2 ± 0.12 mag in the F110W filter and 1.7 ± 0.2 mag in the F170M filter. We have used our observations of 2M0045 to derive aperture corrections in both filters; correcting to a 15 pixel radius, we derive magnitudes of $m_{110} = 15.44 \pm 0.06$ and $m_{170} = 13.69 \pm 0.06$ for 2M2252A and $m_{110} = 16.65 \pm 0.2$ and $m_{170} = 15.35 \pm 0.2$ for 2M2252B. As before, the magnitudes are tied to the Vega flux zero points.

Combining these magnitude estimates, we derive $m_{110} = 15.43 \pm 0.07$, $(m_{110} - m_{170}) = 1.74 \pm 0.1$ for 2M2252A and $m_{110} = 16.55 \pm 0.15$, $(m_{110} - m_{170}) = 1.3 \pm 0.2$ for 2M2252B. The bluer infrared colors for the fainter component suggest that 2M2252B is either a background K/early-M star, or a companion T dwarf. A star of this spectral type would be expected to have relatively blue optical/near-infrared colors, $(R - J) \sim 1.5$ and $(I - J) \sim 0.7$, or $R \sim 17$ and $I \sim 16.5$. Such an object would be easily visible on sky survey plate material. Inspection of the Digital Sky Survey scans of the UK Schmidt IIIaF (*R*-band) plate of this field shows no optical counterpart ($R < 21.5$) within $10''$ of the current position; this argues against 2M2252B being a background star. 2M2252 itself is visible on the scans of the IVN (*I*-band) plate with a magnitude close to the plate limit, $I \sim 18.5$.

2.3. Photometric Calibration

Our measurements of 2M2252A/B are made with the *HST* F110W and F170M filters. For comparative purposes, it is useful to transform these measurements to the standard *J* and *H* passbands. The F110W filter encompasses the *J* band, extending to shorter wavelengths, with a cutoff at $\sim 0.8 \mu\text{m}$, while the F170M filter is centered on the $1.6 \mu\text{m}$ methane feature. We have calibrated the relation between the two magnitude systems using two methods.

First, we have compiled aperture photometry for single (or at least unresolved) ultracool dwarfs with spectral types between

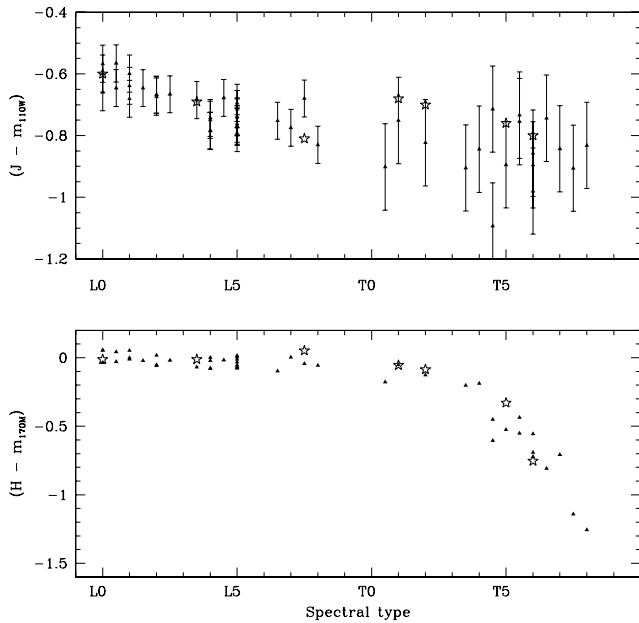


FIG. 2.—Color transformations as a function of spectral type for L and T dwarfs. The top panel plots $(J - m_{110})$ as a function of spectral type, and the bottom panel plots $(H - m_{170})$; in both cases, the *HST* filter magnitudes are scaled to the Vega flux zero point. Filled symbols mark empirical data from NICMOS observations; open stars show the predicted color terms synthesized from flux-calibrated spectra.

L0 and T8. The L dwarf observations are from our own program (No. 10143), while the T dwarf data are from Burgasser’s program (No. 9833). All of the observations were taken with the NIC1 camera, and the measurements were made using an aperture of radius 15 pixels. The typical formal uncertainties in the photometry (both passbands) are ± 0.05 mag for the L dwarf observations and ± 0.15 mag for the fainter T dwarfs. As before, the magnitudes are scaled to Vega flux zero points.

We have also used the IRAF SYNPHOT package to compute relative F110W and F170M count rates from flux-calibrated spectra of L and T dwarfs. The flux-calibrated spectra combine near-infrared (1.0–2.5 μm) UKIRT Cooled Grating Spectrometer 4 (CGS4) data (Geballe et al. 2002; Reid et al. 2001a) with Keck Low-Resolution Imaging Spectrometer (LRIS) spectra (Kirkpatrick et al. 2000; Burgasser et al. 2003a) covering 0.6–1.0 μm . All spectra were normalized to the same apparent magnitude, at either J (for the F110W measurements) or H (F170M), and the CALCPHOT routine was used to predict the observed count rate in the *HST* filter system. The ratio between the count rates predicted for different ultracool dwarfs gives the F110W/ J and F170M/ H color terms as a function of spectral type.

All of the ultracool dwarfs with *HST* NICMOS data have 2MASS JHK_s photometry. Figure 2 shows $(J - m_{110})$ and $(H - m_{170})$ for those sources as a function of spectral type. We have scaled the CALCPHOT measurements to spectral type L0, and the predicted colors are also shown in Figure 2 (*open stars*). The two sets of estimates are in reasonable agreement. Considering the relative magnitudes of binary components, an L or T companion has a larger magnitude difference at F110W than J . Relative to an L0 primary [i.e., $\delta(\text{spectral type}) = 10$ for a T0 companion],

$$(J_1 - J_2) = \delta(J) \approx \delta(\text{F110W}) - 0.02\delta(\text{spectral type}),$$

spectral type < T0,

and

$$\delta(J) \approx \delta(\text{F110W}) - 0.2, \quad \text{spectral type} \geq \text{T0}.$$

These trends probably reflect the growing strength of the 1.1 μm water band, which affects F110W more than the J band. At F170M, $\delta(H) \sim \delta(\text{F170M})$ to T4, with the F170M magnitude becoming progressively fainter at later spectral types as the 1.6 μm methane band strengthens.

2.4. Infrared Spectroscopy

Kendall et al. (2004) used CGS4 on UKIRT to obtain near-infrared spectra of 2M2252, covering the H and K passbands. They estimate a spectral type of L7.5 based on matching those data against observations of spectral standards. In the case of 2M2252, they find best agreement with the L7 template in the H band and the L8 template at K (see their Fig. 2). There is a suggestion of an absorption feature at 1.67 μm in their H -band spectrum of 2M2252, although both that spectrum and their spectra of earlier type dwarfs appear to have spurious (possibly instrumental?) features between 1.55 and 1.65 μm .

More recently, McGovern (2005) obtained moderate-resolution J -band spectra of 2M2252 using NIRSPEC on the Keck telescope. McGovern identified 2M2252 as a possible binary on the basis of unusual band strengths similar to those of the ultracool multiple system DENIS-P J0205.4–1159 (DENIS 0205–11). Bouy et al. (2005) have reanalyzed *HST* WFPC2 observations of the latter system, and they suggest that the fainter component is itself a close binary, comprising an L8 and a T0. They assign a spectral type of L5.5 to DENIS 0205-11A.

We have obtained low-resolution spectroscopy of 2M2252 using the Spex infrared spectrograph (Rayner et al. 2003) on the NASA IRTF. The data were acquired on 2005 August 10 (UT) under nonphotometric conditions but with moderate seeing (0'7 to 0'9). The observations were made in prism mode with a 0'5 slit, giving wavelength coverage from 0.7 to 2.5 μm at a resolution of $R \sim 150$. The data were reduced and calibrated using the SpeXtool calibration package (Cushing et al. 2004), as described in Burgasser et al. (2004); terrestrial absorption features were removed using observations of the nearby A0 V star, HD 222332.

Figure 3 compares our flux-calibrated observations of 2M2252 against data for SDSS J042348.57–041403.5 (SDSS 0423–0414) (Burgasser et al. 2004). SDSS 0423 is the archetype for spectral type T0 (Geballe et al. 2002), exhibiting weak methane absorption in the H passband. That system has also been classed as spectral type L7.5 based on its optical spectrum (Cruz et al. 2003). Recent *HST* observations with NICMOS show that the system is binary, probably consisting of a late-type L dwarf and an early-type T dwarf (Burgasser et al. 2005b). 2M2252 clearly has a very similar spectral energy distribution, with strong H_2 absorption at 1.1 μm and mild methane absorption. In particular, the 1.63 and 1.67 μm $2\nu_2 + \nu_3$ and $2\nu_3$ band heads of CH_4 , which were hinted at in the Kendall et al. (2004) CGS4 data, are clearly present in our Spex data. The $\nu_2 + \nu_3$ methane band is also present at 2.2 μm . Synthesizing these various photometric and spectroscopic observations, we conclude that 2M2252B is a T-type companion of the late-type L primary, 2M2252A.

3. THE 2M2252 SYSTEM

Can we be more specific as to the likely spectral types of the components in the 2M2252 system? We can use our NICMOS

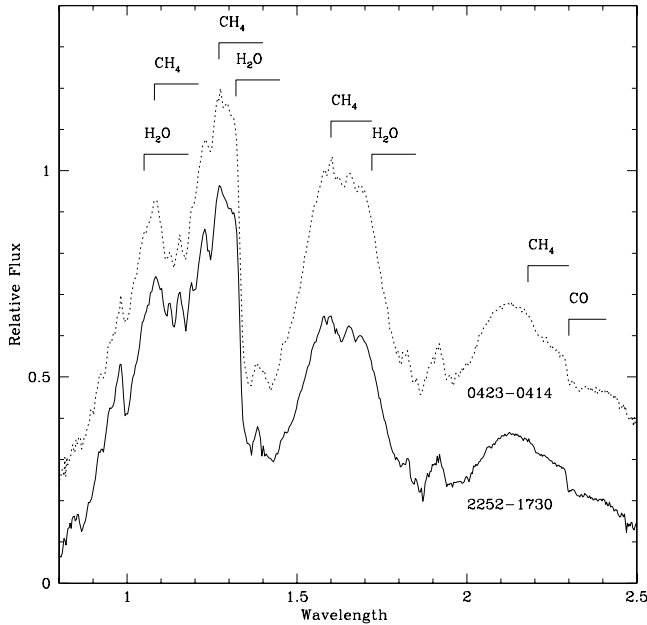


FIG. 3.—Low-resolution infrared spectra of 2M2252 (from our observations) and of SDSS 0423–0414, the T0 archetype (from Burgasser et al. 2004). We have marked the location of molecular absorption bands due to H₂O, CO, and CH₄. Both SDSS 0423 and 2M2252 systems are binaries (see Burgasser et al. 2005b for SDSS 0423), and both exhibit weak but definite CH₄ absorption in the *H* band.

photometry to estimate spectral types for the individual components. The top panel in Figure 4 plots ($m_{110} - m_{170}$) colors as a function of spectral type; the bottom panel shows ($J-H$) colors (for the same systems) as a comparison. The horizontal boxes (*A* and *B*) mark our measurements of 2M2252A and 2M2252B, respectively. These are consistent with spectral types L5–T0 for the primary and T1–T4 for the secondary.

The magnitude difference between the two components favors a spectral type of T0–T2 for the fainter dwarf. One of the more surprising discoveries of recent years is that mid-type T dwarfs have brighter absolute magnitudes in the *J* band than late-type L dwarfs (see Fig. 2 in Vrba et al. 2004). We measure a magnitude difference of $\Delta J \approx 1.0$; this argues against a spectral type later than T3 for the companion, since that would require the primary to have a spectral type earlier than L5. 2M2252B therefore probably lies near the first minimum in the (M_J , spectral type) diagram for ultracool dwarfs.

The near-infrared spectrum of 2M2252 argues for an early-type T dwarf companion. The ultracool dwarf, 2MASS 05185995–2828372 (2M0518), has been identified as an unresolved L/T binary on the basis of the unusual band strengths in its infrared spectrum; while the *K*-band spectrum is consistent with a late L dwarf (CO and pressure-induced H₂ absorption), there is extremely strong H₂O absorption in the *J* band and moderate methane absorption at 1.6 μm (Cruz et al. 2004). The observed features in 2M0518 can be reproduced by combining an L6 dwarf and a T4 dwarf and assigning the two components equal magnitudes at *J* (see Cruz et al. 2004, Fig. 3).

In contrast, Figure 5 compares our spectrum of 2M2252 against composite spectra derived by combining IRTF Spex observations of spectral standards, scaling the latter to the appropriate relative flux level at F110W. The main spectral features (H₂O in *J*, CH₄ in *H* and *K*) are best matched by either the L6+T2 or L6+T3 composites, although both combinations plotted here have significantly redder ($J-H$) and ($H-K$) colors

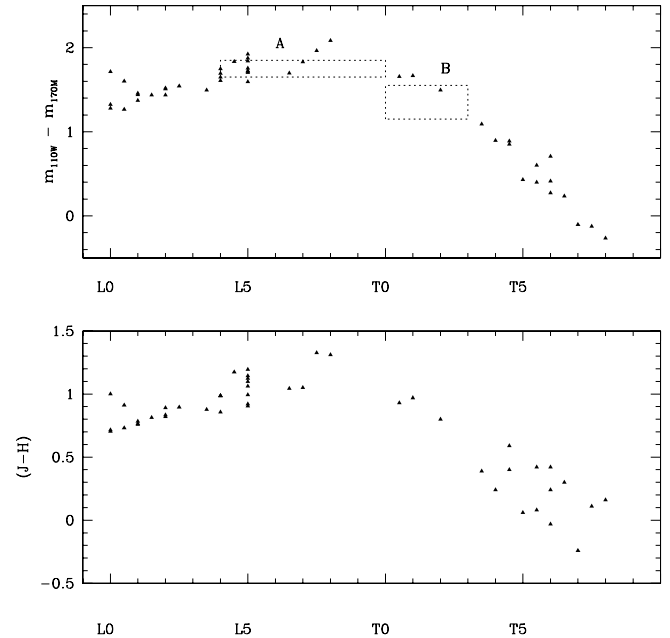


FIG. 4.—Near-infrared colors as a function of spectral type for L and T dwarfs: the top panel plots ($m_{110} - m_{170}$) colors (filled triangles); the bottom panel plots ($J-H$) colors (filled triangles) for the same sources, as a reference comparison. The dotted boxes in the top panel outline the spectral types that are consistent with the colors measured for the two components of 2M2252.

than 2M2252; the L7+T4 composite is much closer to the overall spectral shape but produces much stronger CH₄ and H₂O absorption than observed. Ultracool dwarfs, particularly L dwarfs, display a range of near-infrared colors at any given spectral type, a characteristic that is usually ascribed to variations in the atmospheric dust content. 2M2252 may include a particularly dust-free L dwarf component.

The infrared spectroscopy, near-infrared colors, and the observed magnitude difference all set constraints on the spectral types of the ultracool dwarfs in the 2M2252B system. Combining those constraints, the most likely scenario, on balance, is that 2M2252 consists of an L6 \pm 1 primary ($M_J \sim 14$) and T2 \pm 1 secondary ($M_J \sim 15$).

4. DISCUSSION

Kendall et al. (2004) estimated a distance of 8.3 pc for 2M2252 based on a spectral type of L7.5 and the spectral-type/ M_J correlation from Cruz et al. (2003).⁶ Adopting a spectral type of L6 for the primary implies $M_J = 14$. Given the spectral types estimated in the previous section, we can transform the F110W/F170M measurements to *J*, *H* photometry. Figure 2 shows $J \sim \text{F110W} - 0.75$ for 2M2252A, and $J \sim \text{F110W} - 0.9$ for 2M2252B, while $H \sim \text{F170M} - 0.05$ for both systems. Allowing for uncertainties in the transformation, the corresponding magnitudes and colors are $J = 14.67 \pm 0.09$, ($J-H$) = 1.05 ± 0.10 for 2M2252A and $J = 15.65 \pm 0.15$, ($J-H$) = 0.45 ± 0.2 for 2M2252B. In that case, the distance modulus is 0.7 ± 0.5 mag, giving a revised distance of $13.6^{+3.8}_{-2.6}$ pc.

At present, we lack high signal-to-noise ratio optical spectroscopy and, as a result, have no direct evidence (through lithium detection) whether 2M2252A has a mass exceeding $0.06 M_{\odot}$. However, assuming spectral types of L6 and T2, both components

⁶ This approach is not strictly correct, since the spectral type is derived from spectroscopy in the *H* and *K* passbands, while the Cruz et al. (2003) calibration is appropriate to optical spectral types.

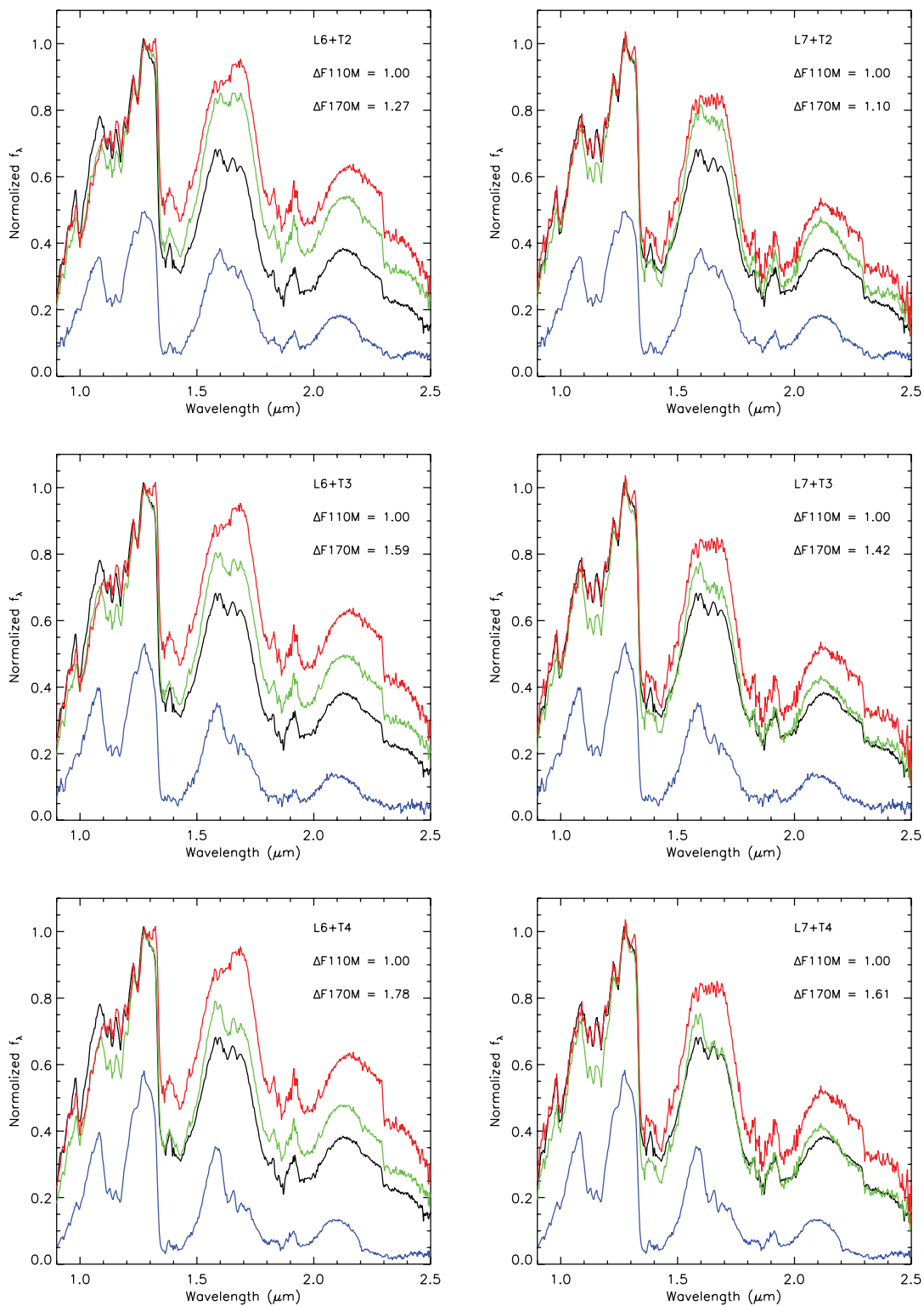


FIG. 5.—Comparison between the observed spectrum of 2M2252 and composite spectra, made by combining IRTF Spex spectra of spectral templates. In each panel, the uppermost (*red*) spectrum is the L dwarf, the lowest (*blue*) spectrum is the T dwarf, the combined spectrum is plotted in green, and the actual observations of 2M2252 are plotted in black. The L/T flux F110W ratios are set to 2.5:1 ($\delta F_{110W} = 1.0$ mag) in each composite spectrum, and the corresponding magnitude difference at F170M is shown in the figure. The L6/T3 composite gives the closest match morphologically to 2M2252 at *H* and *K*, although the depth of H_2O absorption at F110W is overpredicted; however, 2M2252 is bluer in (*J*–*H*) and (*H*–*K*) than all save the L7/T4 composite. The spectral templates are 2MASS 1010–0406 (L6), Denis 0205 (L7), SDSS 1254–0122 (T2), 2MASS 1209–10004 (T3), and 2MASS 2254+3123 (T4).

of 2M2252 are likely to be brown dwarfs with effective temperatures of ~ 1500 and ~ 1300 K, respectively (Golimowski et al. 2004). Evolutionary models of low-mass dwarfs predict that $T_{\text{eff}} \propto \tau^{-0.32} M^{0.83}$ (Burrows et al. 2001), where τ is the age. Assuming that both components are coeval, the mass ratio predicted for the 2M2252 system is $M_2/M_1 \approx 0.84$. This high mass ratio is consistent with data for most known ultracool binaries.

The projected separation between the two components is only 1.77 AU (for a distance of 13.6 pc). Statistically, the most likely semimajor axis is 126% of the observed separation (Fischer & Marcy 1992), or $\langle a \rangle = 2.2$ AU; while Torres (1999) has demonstrated that 85% of binary systems have semimajor axes between one-half and twice the observed separation. If we assume masses of $0.07 M_{\odot}$ and $0.06 M_{\odot}$ for the two components ($M_{\text{tot}} = 0.13 M_{\odot}$) and $a = 2.2$ AU, the binary system has a period of ~ 9.1 yr; for $M_{\text{tot}} = 0.06 M_{\odot}$, the period is 13.3 yr. Applying the Torres formalism, there is an 85% probability that the period lies between 25.6 and 3.2 yr for $M_{\text{tot}} = 0.13 M_{\odot}$, or 37.7 and 4.7 yr for $M_{\text{tot}} = 0.06 M_{\odot}$.

5. SUMMARY

HST NICMOS observations of 2MASS J22521073–1730134 (2M2252) show that this ultracool dwarf is a binary system. Both the near-infrared colors and 1–2.5 μm spectroscopy indicate that the companion is an early-type T dwarf. Based on the colors and relative magnitudes measured in the F110W and F170M filters, we identify 2M2252A as a late-type L dwarf, probably of spectral type $L6 \pm 1$, and 2M2252B as an early-type T dwarf, with spectral type T2/T3.

With the addition of 2M2252, there are now five ultracool dwarfs that are probably late-L/early-T binaries. One system, 2MASS J0518 (Cruz et al. 2004), is unresolved; in two other systems, Denis 0205-11B (Bouy et al. 2005) and Gl 337CD (Burgasser et al. 2005a), the binary components are only barely resolved. The fourth system, SDSS 0423-0414, is very similar to 2M2252, with the late-L and early-T components separated by 2.45 AU (Burgasser et al. 2005b). Further high-resolution observations of these systems, particularly 2M2252 and SDSS 0423-0414, offer the prospect of mapping the astrometric orbits, yielding dynamical masses that can be used to constrain evolutionary models of the L/T transition.

The observations described in this paper are associated with *HST* programs 10143 and 9833, and those data were obtained via the *Hubble Space Telescope* data archive facilities maintained at the Space Telescope Science Institute. Support for this research was provided by NASA through a grant from the Space Telescope Science Institute, which is operated by the Association of Universities for Research in Astronomy, Inc., under NASA contract NAS 5-26555. A. J. B. acknowledges support from NASA through the Spitzer Fellowship Program, and K. L. C. is supported by an NSF Astronomy and Astrophysics Postdoctoral Fellowship under award AST-0401418. Thanks to Michael Liu and Davy Kirkpatrick for useful comments on a draft version of this paper and to Anton Koekemoer for advice in using the SYNPHOT package.

REFERENCES

- Bouy, H., Brandner W., Martín, E.L., Delfosse, X., Allard, F., & Basri, G. 2003, *AJ*, 126, 1526
- Bouy, H., Martín, E. L., Brandner, W., & Bouvier, J. 2005, *AJ*, 129, 511
- Bouy, H., et al. 2004, *A&A*, 423, 341
- Burgasser, A. J., Kirkpatrick, J. D., Liebert, J., & Burrows, A. 2003a, *ApJ*, 594, 510
- Burgasser, A. J., Kirkpatrick, J. D., & Lowrance, P. J. 2005a, *AJ*, 129, 2849
- Burgasser, A. J., Kirkpatrick, J. D., Reid, I. N., Brown, M. E., Miskey, C. L., & Gizis, J. E. 2003b, *ApJ*, 586, 512
- Burgasser, A. J., McElwain, M. W., Kirkpatrick, J. D., Cruz, K. L., Tinney, C. G., & Reid, I. N. 2004, *AJ*, 127, 2856
- Burgasser, A. J., Reid, I. N., Kirkpatrick, J. D., Leggett, S. K., Liebert, J., & Burrows, A. 2005b, *ApJ*, submitted
- Burrows, A., Hubbard, W. B., Lunine, J. I., & Liebert, J. 2001, *Rev. Mod. Phys.*, 73, 719
- Cruz, K. L., Burgasser, A. J., Reid, I. N., & Liebert, J. 2004, *ApJ*, 604, L61
- Cruz, K. L., Reid, I. N., Liebert, J., Kirkpatrick, J. D., & Lowrance, P. J. 2003, *AJ*, 126, 2421
- Cushing, M. C., Vacca, W. D., & Rayner, J. T. 2004, *PASP*, 116, 362
- Fischer, D. A., & Marcy, G. W. 1992, *ApJ* 396, 178
- Geballe, T. R., et al. 2002, *ApJ*, 564, 466
- Gizis, J. E., & Reid, I. N. 2006, *AJ*, 131, 638
- Gizis, J. E., Reid, I. N., Knapp, G. R., Liebert, J., Kirkpatrick, J. D., Koerner, D. W., & Burgasser, A. J. 2003, *AJ*, 125, 3302
- Golimowski, D. A., et al. 2004, *AJ*, 127, 3516
- Kendall, T. R., Delfosse, X., Martín, E. L., & Forveille, T. 2004, *A&A*, 416, L17
- Kirkpatrick, J. D., et al. 2000, *AJ*, 120, 447
- McGovern, M. 2005, Ph.D. thesis, Univ. of California, Los Angeles
- Rayner, J. T., Toomey, D. W., Onaka, P. M., Denault, A. J., Stahlberger, W. E., Vacca, W. D., Cushing, M. C., & Wang, S. 2003, *PASP*, 115, 362
- Reid, I. N., Burgasser, A. J., Cruz, K. L., Kirkpatrick, J. D., & Gizis, J. E. 2001a, *AJ*, 121, 1710
- Reid, I. N., Gizis, J. E., Kirkpatrick, J. D., & Koerner, D. W. 2001b, *AJ*, 121, 489
- Torres, G. 1999, *PASP*, 111, 169
- Vrba, F. J., et al. 2004, *AJ*, 127, 2948
- Zapatero Osorio, M. R., Lane, B. F., Pavlenko, Y., Martín, E. L., Britton, M., & Kulkarni, S. R. 2004, *ApJ*, 615, 958